

Performance of Self-Compacting Concrete Confined using GFRP and Subjected to Compression Loading

Tarek Bahaa

Building Material and Quality Control Institute, Housing and Building National Research Center, Cairo, Egypt
tarekbaha@yahoo.com

Abstract: This research investigates and evaluates the behavior of self-compacting concrete (SCC) confined in glass fiber reinforced polymer (GFRP) tubes and subjected to axial compression loading. The experimental program included testing of eleven specimens loaded in compression until failure. Seven specimens were subjected to axial loading while four specimens were subjected to eccentric loading. The experimental program is designed to demonstrate the effect of main variables that include : the confinement of GFRP tube, the percentage of longitudinal reinforcement, the diameter of the GFRP tube, the concrete compressive strength and the load eccentricity. The discussion of test results included cracking behavior; failure mode; the load-strain response; and the strains in GFRP tubes. Strength gain and the deformability were used to evaluate the behavior of the tested specimens. The results showed notable enhancement in the structural behavior of SCC due to confinement using GFRP tube. Gain in strength up to 50% and 37% was achieved for plain and steel reinforced SCC, respectively. Increasing the compressive strength of concrete by 81% resulted in only 59% increase in the specimen ultimate load. The evaluated behavior displayed that the improvement in the strength for the axially loaded specimens is more pronounced than specimens subjected to eccentric loading. For specimens subjected to eccentric loading, load eccentricity was found to have a significant effect on the performance of SCC confined by GFRP. It reduced the ultimate capacity while it enhanced the deformability.

[Tarek Bahaa. **Performance of Self-Compacting Concrete Confined using GFRP and Subjected to Compression Loading.** *J Am Sci* 2013;9(12):863-872]. (ISSN: 1545-1003). <http://www.jofamericanscience.org>. 110

Keywords: Self-Compacting Concrete, FRP, Confinement, Compression, Deformability, eccentricity.

1. Introduction

Self-compacting concrete (SCC) is a new generation of concrete that can be compacted under its own weight without the need of external vibration. It is characterized by its ability to flow and fill narrow and deep members and produces uniform and integrated concrete members without any sign of segregation or bleeding. This performance can not be achieved through utilizing the conventional normal concrete. Researches were made to determine and evaluate the properties of self-compacting concrete. Based on these researches, specifications were issued for self-compacting concrete [1] and the use of SCC in several applications such as slender columns, deep beams, retaining walls and piles has increased.

Fiber reinforced polymers (FRP) has been proved to be an effective technique for external confinement of reinforced concrete axially loaded members. It has some advantages over the conventional steel confinement. Confinement with FRP is easier and faster in construction, produces lighter and smaller size sections and results in minor change in the stiffness of the member. Several studies investigated experimentally the confinement of conventional concrete using FRP for both normal and high strength concrete [2&3]. Results showed significant enhancement in strength and deformability of the axially loaded specimens due to confinement. On the other hand, theoretical models

have been developed to determine the enhancements in strength and ductility of concrete members confined by FRP and subjected to compression loading [4&5].

The confinement of SCC using FRP produces high performance structural members that has higher carrying capacity and is protected from aggressive environments such as seawater and salts in soil, i.e. corrosion resistant. One of the innovative confinement methods is casting SCC into FRP tubes. The FRP tubes serve a three-fold function of working as a stay-in-place formwork, confinement of concrete and protecting the member from external aggressive environments. Few studies addressed the structural behavior of SCC confined with FRP tubes and subjected to compression loading [6]. Significant improvements in strength and deformability of the FRP confined SCC while marginal effect on stiffness was reported.

The current study is intended to investigate and evaluate the performance of self-compacting concrete confined using GFRP tubes and subjected to compression loading. Confinement is achieved through casting SCC in locally produced GFRP tubes. The experimental program is designed to demonstrate the effect of main variables that include : the confinement of FRP tube, the percentage of longitudinal reinforcement, the diameter of the GFRP

tube, the concrete compressive strength and the load eccentricity.

2. Experimental Program

2.1 Material Properties

The fine aggregate used in the concrete mixes is siliceous sand with a specific weight of 2.65 and percentage of absorption of 0.40%. The coarse aggregate is size no 1 crushed dolomite, i.e. a maximum nominal size of 10 mm. Its specific weight equals 2.50 and the percentage of absorption equals 1.2%. The cement is CEM I-42.5N that satisfies the requirements of the Egyptian Standard Specification ESS 4756-1 [7]. Lime stone powder is added to the normal strength concrete mix as a filler material in order to achieve the needed paste volume to produce self-compacting concrete. The powder has a specific weight of 2.50 and a fineness of 4050 cm²/gm.

A modified polycarboxylate polymer superplasticizer namely Sika ViscoCrete 5400 that satisfy the requirements for ASTM C-494 types A and F [8] was used. It produces high flowability of the mix while preserving its viscosity. It had a specific weight of 1.10. SCC has a high content of cementitious material that develops shrinkage values higher than that of the conventional concrete. To overcome this side effect, an expanding agent namely Intraplast Z was used to produce a slow controlled expansion. This ensures full composite action between the tube and concrete. Silica fume was utilized as 15% addition of the cement weight to produce the high strength concrete mix. The silica has a specific weight of 2.10 and a specific surface area of 20 m²/gm.

Locally produced GFRP tubes obtained from the Future Pipe Industries Company, Egypt are used to

cast and confine SCC. The average tensile strength of the GFRP tubes obtained from ring specimen tests equals 77 N/mm². Mild steel smooth bars of 6 mm diameter, yield strength of 320 N/mm² and ultimate strength of 440 N/mm² were used for spiral transverse reinforcement. Deformed high tensile steel bars of 10 and 12 mm diameter, yield strength of 460 and 490 N/mm² and ultimate strength of 680 and 720 N/mm², respectively, were used for longitudinal reinforcement.

2.2 Design of the SCC Mixes

The SCC mixes were designed using the Egyptian Technical Specifications for SCC [1]. The guidelines reported in the specification were used for proportioning an initial trial mix. The mix was visually examined for signs of segregation or bleeding. The performance of the mix in the fresh state was evaluated and hence proportions were adjusted till satisfying the self-compactability requirements. Table 1 gives the quantities of materials required for one cubic meter of normal strength and high strength SCC mixes. The performance of the mix in the fresh state was evaluated using the slump flow and V-funnel tests. The compressive strength of the mix was determined through testing 158x158x158 mm concrete cubes. Moreover, prisms were cast to perform the dry shrinkage test [9] and the volume change was estimated at age of 7, 14 and 28 days. Table 2 gives the properties of the SCC mixes. The positive values of the shrinkage test indicate that the specimen displayed expansion and so the tube perfectly confines concrete.

Table (1): Composition of One Cubic Meter of the SCC Mixes (kg)

Constituent Mix	Cement	Silica Fume	Limestone Powder	Sand	Dolomite	Water	Super- plasticizer	Expanding Agent
Mix 1	450	-	60	810	810	195	5	4
Mix 2	500	75	-	805	805	175	10	5

Table (2): Properties of the SCC Mixes












Test	Mix 1	Mix 2	Specifications Limits[1]
Compressive Strength, Mpa	55.6	100.5	-
Slump Flow	690 mm	630 mm	600 - 800
Flow Time T ₅₀	4.8 Sec	5.0 Sec	2 - 5
V-Funnel Time	8.1 Sec	9.2 Sec	6 - 12
Drying Shrinkage Test:			
At 7 days	+1.70 E-4 mm/mm	+1.30 E-4 mm/mm	-
At 14 day	+1.75 E-4 mm/mm	+1.32 E-4 mm/mm	-
At 28 days	+1.66 E-4 mm/mm	+1.29 E-4 mm/mm	-

2.3 Details and Fabrication of Specimens

The research program comprises testing of eleven specimens subjected to compression loading and designated as C1 to C11. All specimens had a height of 1100 mm and a diameter of 200 mm except specimen C7 that has a diameter of 160 mm. Table 3 presents the concrete compressive strength (f_{cu}), the

longitudinal and transverse reinforcement, the shape of the cross section, the load eccentricity, if any, and description of the specimen. The tubes were sealed from their bottom ends and fixed in a vertical position then filled with SCC from their upper ends. Specimens were cured in the lab by covering their upper ends with wet burlap for 28 days.

Table (3): Details of the Tested Specimens

Specimen No.	f_{cu} (N/mm ²)	Longitudinal Reinforcement	Transverse Reinforcement	Cross Section	eccentricity e (mm)	Notes
C1	55.6	–	–		0	Plain SCC (PC)
C2	55.6	6#10	5#6/m'		0	Reinforced SCC (RC)
C3	55.6	–	–		0	PC confined by GFRP
C4	55.6	6#10	5#6/m'		0	RC confined by GFRP
C5	55.6	6#12	5#6/m'		0	RC confined by GFRP
C6	100.5	–	–		0	HSC confined by GFRP
C7	55.6	-	-		0	PC confined by GFRP
C8	55.6	6#12	5#6/m'		25	Reinforced SCC (RC)
C9	55.6	–	–		25	PC confined by GFRP
C10	55.6	6#12	5#6/m'		25	RC confined by GFRP
C11	55.6	6#12	5#6/m'		40	RC confined by GFRP

2.4 Test Setup and Instrumentation

The specimens were tested up to failure using an AMSLER compression testing machine of 5000 kN capacity. The testing machine consists of lower moving piston on a spherical head covered by a rigid steel plate. The upper plate is moving around a fixed sphere. This ensures that the applied load is always passing through the center and perpendicular to the specimen cross section for concentric specimens, i.e. axial compression. The ends of the specimen are confined by steel rings to prevent any premature failure at loading points. Two ball seating were provided at top and bottom of the specimens to allow the application of the required eccentricity, (if any). Figure 1 shows test setup and instrumentation of the specimens.

A 5000 kN electrical load cell was used to measure the applied load. Longitudinal deformations of the specimens were measured using two linear variable displacement transducers, (LVDTs) over a length of 300 mm mounted as shown in Figure 2 and fixed in the concrete core. An additional LVDT was positioned at the mid height of the specimen to record the lateral horizontal displacement. Moreover, the specimens were instrumented to record the horizontal and vertical strains developed in the GFRP tube using 10 mm electrical strain gages. The readings of the measuring devices, i.e. load cell, LVDTs and electrical strain gages were read, transformed and stored as forces, displacements and micro-strains, respectively, by means of a data logger system and stored in a computer.

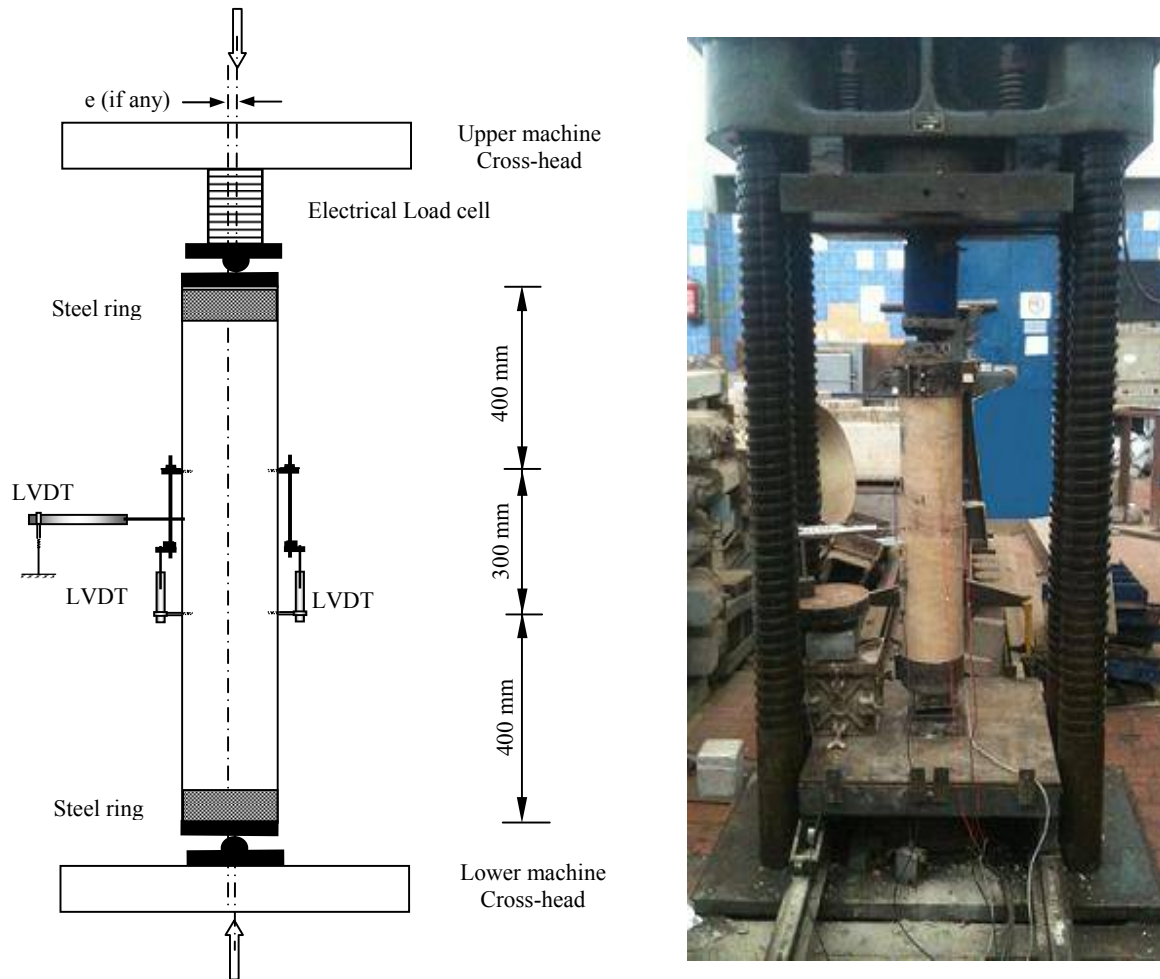


Figure (1): Test Setup and Instrumentation

3. Test Results

3.1 Cracking and Mode of Failure

The unconfined plain SCC specimen C1 experienced vertical cracks in the middle zone then sudden failure occurred on inclined shear sliding plane. The steel reinforced SCC specimens C2 and C8 showed the typical cracking behavior of RC axially loaded and eccentrically loaded members, respectively. The spread of vertical cracks was more obvious before spall of the concrete cover then failure due to crushing of the concrete in compression and buckling of longitudinal reinforcement took place.

On the other hand, the axially loaded plain SCC specimens confined by GFRP, C3 to C7, did not show visible deformations till higher levels of loading where white marks were observed on the GFRP tube indicating development of high stresses in

fibers. Near ultimate load, fracture sound of fibers was progressive till sudden failure occurred due to cut in the GFRP tube and crushing of the concrete core, refer to Figure 2. It is worth mentioning that the failure of specimen C6 occurred in a more sudden and explosive fashion due to the known brittleness of high strength concrete.

On the other side, the behavior of the GFRP-confined SCC specimens which are subjected to eccentric loading, C9 to C11, was similar to their counter part axially loaded specimens at early stages of loading. Upon loading, the glass fibers continue to fracture. At ultimate level, the GFRP tube crushed in the compression side and ruptures in the tension side and simultaneously the concrete core crushed in compression.

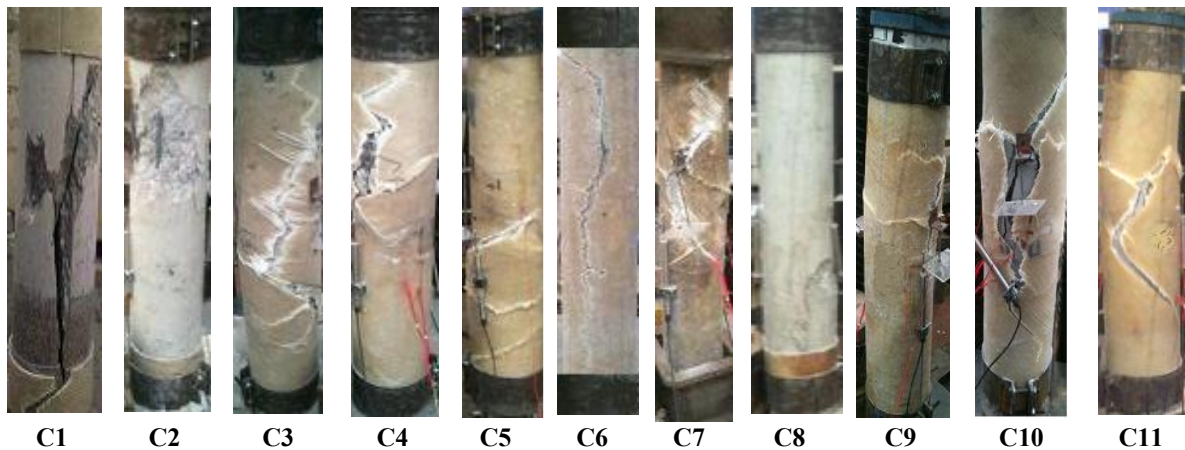


Figure (2): Appearance of the Specimens after Testing

3.2 Longitudinal Load-Deformation Results

The ultimate load and the developed axial deformation in the middle region over a length of 300 mm were determined for the tested specimens. Table 4 introduces the main test results. It should be explained that for the axially loaded specimens, the longitudinal deformation values given in the table represent the average value of the longitudinal compression deformations measured on the two sides of each specimen, i.e. axial deformations. On the other hand, for the eccentrically loaded specimens, the longitudinal deformation values given in the table represent the longitudinal compression deformation measured on the specimen side that is subjected to compression stresses throughout the test.

The HSC GFRP-confined specimen C6 recorded the highest ultimate capacity among the tested specimens that equals 3846 KN while the unconfined specimen C1 recorded the lowest ultimate load value of 1607 KN and the lowest axial compression deformation at ultimate load of 0.177 mm. For the axially loaded specimens, specimen C5 experienced the highest axial deformation of 1.344 mm. On the other hand, specimen C11 has the highest longitudinal compression deformation of 7.629 mm among the specimens subjected to eccentric loading. The load-deformation response will be critically examined through comparing the load-strain curves of the tested specimens when evaluating the effect of main variables in section 4.

Table (4): Test Results

Specimen	Ultimate Load, P (KN)	Longitudinal Compression Deformation at Ultimate Load (mm)	Mid-Height Lateral Displacement (mm)	Strains in GFRP (μ_s)		Longitudinal Strain at Ultimate Load (mm/mm)
				Long.	Lateral	
C1	1607	-0.177	0.549	-	-	-0.00059
C2	1915	-0.336	0.558	-	-	-0.00112
C3	2415	-0.909	1.862	-3664	4730	-0.00303
C4	2625	-1.311	2.244	-5743	4375	-0.00437
C5	2713	-1.344	2.583	-6754	5343	-0.00448
C6	3846	-0.657	1.043	-2139	601	-0.00219
C7	1716	-1.053	3.751	-11948	10109	-0.00351
C8	1611	-0.798	1.816	-	-	-0.00266
C9	1649	-1.407	6.369	*	*	-0.00469
C10	1828	-7.323	12.123	-15745	12829	-0.02441
C11	1621	-7.629	21.713	-26297	25961	-0.02543

* Not Measured

3.3 Mid-Height Lateral Displacement

Table 4 gives the mid-height lateral displacement of the specimens at ultimate load level. In general, the specimens confined with GFRP tubes sustained higher lateral displacement than the unconfined specimens did. Regarding the axially loaded specimens, mid-height lateral displacement ranged from 0.549 mm, for specimen C1, to 3.751 mm, for specimen C7 that has the smaller diameter of 160 mm. These values are an indication of the second order effect for the axially loaded members.

On the other hand, specimens, which are subjected to eccentric loading, normally showed much higher mid-height lateral displacement values that ranged from 1.816 mm to 21.713 mm for the unconfined specimen C8 and the confined specimen C11, respectively. This increase in the lateral displacement resulted from the moment generated by the load eccentricity and the additional moment resulted from the second order effect.

3.4 Strains in GFRP Tubes

At early stages of loading, the measured strains in the GFRP of the confined specimens were relatively small. This indicates that the GFRP at these levels of loading didn't provide effective confinement because the expansion of the concrete core was not enough to strain the GFRP. Approaching the ultimate load level, the lateral strains in the GFRP significantly increased indicating that the GFRP provide high confinement pressure on the concrete core of the specimens.

Despite that the GFRP tube was not loaded and the load was applied on the concrete core area, compression strains were developed in the longitudinal direction of the GFRP tubes. These strains were transferred from the concrete core to the GFRP through friction and confirmed the good bond between the GFRP and the concrete.

Table 4 presents the longitudinal compressive and the lateral tensile strains developed at ultimate load in the GFRP for the confined specimen. Referring to the results of the axially loaded specimens, the HSC confined specimen, C6, possessed the lowest longitudinal and lateral strain values of $-2139 \mu_s$ and $601 \mu_s$, respectively. This can be explained through the fact that HSC has less deformability and higher modulus of elasticity. On the contrary, the specimen confined by the small diameter GFRP tube, $D=160\text{mm}$, displayed the highest longitudinal and lateral strains of $-11948 \mu_s$ and $10109 \mu_s$, respectively. This indicates that GFRP was considerably strained and provided effective confinement pressure on the SCC core.

The specimens subjected to eccentric loading displayed higher longitudinal compressive and lateral

tensile strains up to $-26297 \mu_s$ and $25961 \mu_s$, respectively, for specimen C11. This is logical since the specimens are subjected to combined axial and bending moment that is characterized by its higher deformations than pure axial loading. After ultimate load, records showed increase in the GFRP strains till the strain gage broke down.

4. Effect of Main Test Variables

In the following subsections, the effect of main variables on the structural behavior of the tested specimens will be investigated through comparing their axial load-strain responses. The discussion will shed light on the gain in strength of the specimens confined using GFRP compared to the unconfined specimen. Also, deformability of the specimens will be assessed through the values of longitudinal strain at ultimate load, see Table 4. It should be reminded that for axially loaded specimens, the longitudinal strain values given in the Table 4 or plotted in the figures represent the axial strain that is estimated as the average strain value of the two sides of the specimen. On the other hand, for the eccentrically loaded specimens, the longitudinal strain values given in the Table 4 or plotted in the figures represent the longitudinal compression strain of the specimen side that is subjected to compression stresses throughout the test.

4.1 Effect of Confinement with GFRP Tube

Confinement is reported to have a favorable effect on the behavior of compression loaded members. In order to evaluate this effect, the behavior of the GFRP confined specimens C3 and C4 will be compared to the unconfined specimens C1 and C2, respectively. Figure 3 and Figure 4 compare the axial load-strain responses for these specimens, respectively.

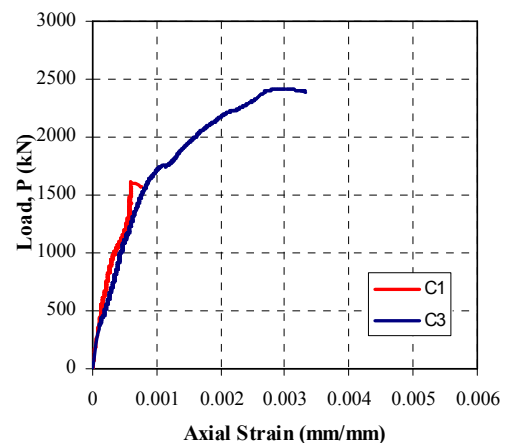


Figure (3): Effect of Confinement of Plain SCC with GFRP

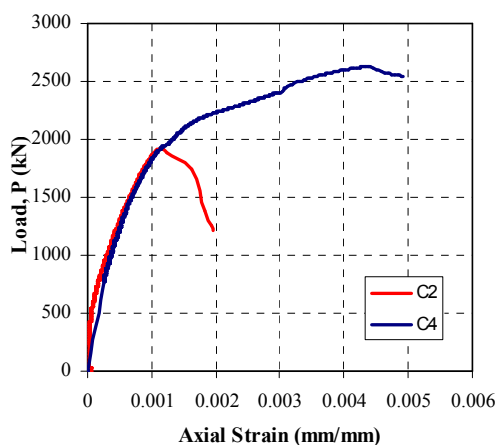


Figure (4): Effect of Confinement of Steel-Reinforced SCC with GFRP

Referring to Figure 3 and results given in Table 4, a notable improvement in the behavior due to confinement with GFRP can be seen. Confining the SCC specimen C3 by GFRP tube resulted in a considerable increase in the ultimate capacity from 1607 kN to 2415 kN, i.e. gain in the strength equals to 50 %. Also, the energy capacity of the specimen C3 improved as indicated by the area under the load-strain curve. In addition, an enormous increase in the deformability, i.e. axial strain at ultimate load level, was found. The GFRP confined SCC specimen C3 recorded an axial strain value of -0.00303 which is about five times that of the unconfined specimen C1.

Similar effects were found in Figure 4 when comparing the behavior of SCC specimens C2 and C4 which are provided with steel reinforcements. Confining the steel-reinforced SCC with GFRP increased the ultimate load by 37%. The deformation capacity of the GFRP confined specimen C4 is about four times that of the unconfined specimen C2 as displayed by the increase of axial strain at ultimate from -0.00112 to -0.00437.

It can be concluded that confinement with GFRP enhances the structural performance of axially load SCC in terms of strength and deformability. The confinement pressure provided by the GFRP enables the concrete core to withstand higher stresses and strains.

4.2 Effect of the Percentage of Longitudinal Reinforcement

The effect of the percentage of longitudinal reinforcement can be evaluated by comparing the behavior of the specimens C3, C4 and C5 as presented in Figure 5. The specimens had longitudinal reinforcement percentage of 0, 1.5 and

2.16%, respectively. The GFRP confined plain SCC without longitudinal reinforcement possessed the lowest strength and deformability of 2415 kN and -0.00303 mm/mm, respectively. Reinforcing the specimen with longitudinal reinforcement of 1.50% and 2.16% increased the ultimate load by 9% and 12%, respectively. On the other side, the deformability showed considerable improvement that equaled 44% and 48%, respectively.

It can be said that the percentage of longitudinal reinforcement has no significant effect on the ultimate capacity of axially loaded SCC confined with GFRP. However, presence of longitudinal reinforcement enhances the deformability as it transforms the behavior from that of brittle plain concrete to the more ductile reinforced concrete. Increasing the percentage of longitudinal reinforcement from 1.50% to 2.16% resulted in marginal increase in both strength and deformability.

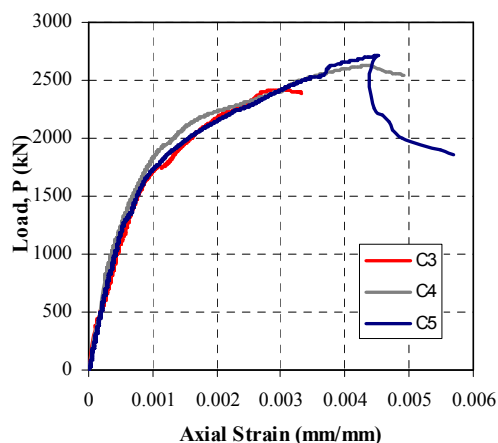


Figure (5): Effect of Percentage of Longitudinal Reinforcement

4.3 Effect of Diameter of GFRP Tube

The effect of the diameter of the GFRP tube can be presented by contrasting the behavior of specimens C3 and C7 in which the tube diameter is 200 mm and 160 mm, respectively. Increasing the tube diameter from 160 mm to 200 mm enhanced the ultimate load from 1716 kN to 2415 kN. This is normal as the ultimate load of axially loaded members is directly proportional to the cross sectional concrete area of the member.

On the contrary, increasing the tube diameter resulted in a reduction in the deformability as indicated by the axial strain values given in Table 4. This is due to the increase of the axial stiffness of the specimen as a result of the increase of the cross sectional area.

For further evaluation of the response, it would be helpful to compare the axial stress-strain response

of specimens C3 and C7 as given in Figure 6. The stress values were estimated through dividing the ultimate load values by the cross sectional area of the concrete member. As seen in Figure 6, reducing the diameter of the GFRP tube enhanced both the strength and deformability of the specimen. The strength was increased from 76.9 N/mm^2 , for C3, to 85.4 N/mm^2 , for C7. In addition, a remarkable enhancement in the ductility of specimen C7 was obtained as seen from Figure 6. Reducing the diameter of the GFRP tube, enables the generated confinement pressure to extend towards the centre of the section and affect larger area of the concrete core. So, the small diameter GFRP tube produces more effective confinement mechanism that enables the axially loaded member to sustain higher stresses and strains.

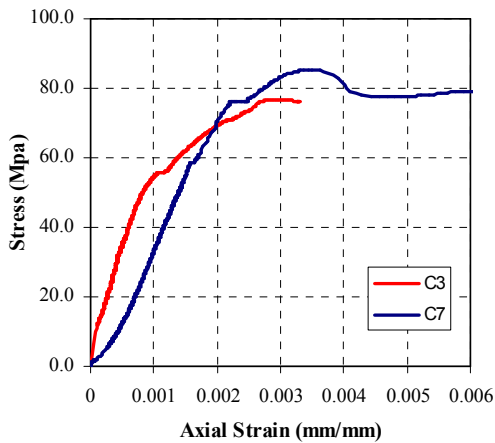


Figure (6): Effect of Diameter of GFRP Tube

4.4 Effect of Concrete Compressive Strength

Figure 7 compares the behavior of specimens C3 and C6 that are identical except their concrete compressive strength that equal 55.6 N/mm^2 and 100.5 N/mm^2 , respectively. As expected, the HSC specimen C6 recorded an ultimate load of 3846 KN which is 59% higher than that of specimen C3. However, it can be noted that the increase in ultimate load was not proportional to the increase in the concrete strength that equaled 81%. This is due to the fact that the higher the strength of concrete, the less lateral expansion of concrete under axial compression. This results in less efficiency of the confinement provided by GFRP.

Referring to Figure 7, as the concrete compressive strength increased, the slope of the ascending branch increased, i.e. higher stiffness. However, increasing the concrete strength reduced the deformability as seen from the axial strain values. This can be attributed to the high modulus of elasticity and lower internal cracking of high strength

concrete. It can be concluded that increasing the concrete compressive strength, increases the ultimate load and stiffness while it reduces the deformability of axially loaded SCC confined by GFRP.

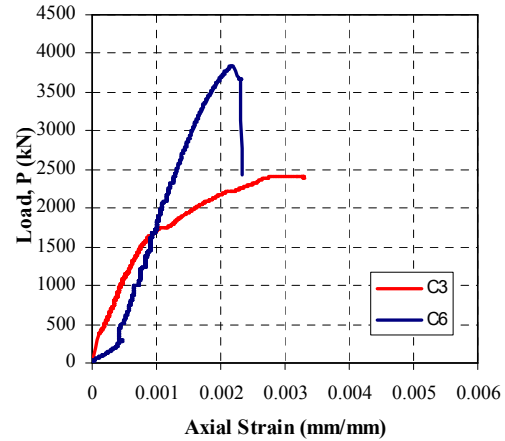


Figure (7): Effect of Concrete Comp. Strength

4.5 Effect of Load Eccentricity

The effect of load eccentricity on the behavior of GFRP confined SCC members was investigated for both plain and steel-reinforced self compacted concrete. Figure 8 compares the load-longitudinal compressive strain relationships for the plain SCC specimens C3 and C9 confined with GFRP and subjected to axial and eccentric loading, $e=25 \text{ mm}$, respectively. The figure together with results in Table 4 reveals the remarkable reduction in the ultimate load from 2415 KN to 1649 KN due to load eccentricity. On the other side, the deformability increased by about 55%. Introducing the eccentricity altered the state of stresses from the pure axial compression loading to the less brittle combined axial compression and bending loading. The later is characterized by its lower load carrying capacity and less sudden failure mechanism.

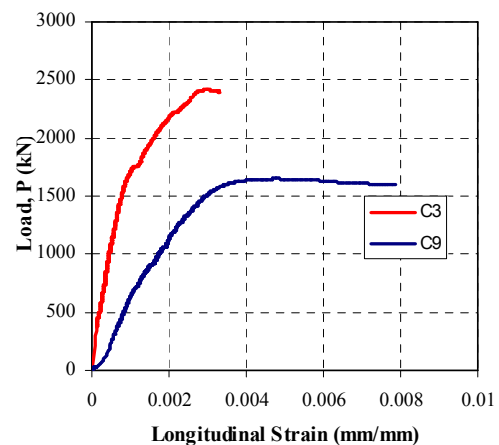


Figure (8): Effect of Load Eccentricity on Plain SCC Confined by GFRP

Similarly, Figure 9 compares the load-longitudinal compressive strain relationships for the steel-reinforced SCC specimens C5, C10 & C11 confined with GFRP and subjected to load eccentricity of 0, 25 mm and 40 mm, respectively. The introduction of eccentricity caused significant change in the response. It reduced the specimen stiffness as demonstrated by the ascending branch of the load-strain response. Also, increasing the load eccentricity from 0 to 25 mm and 40 mm reduced the ultimate load by 33% and 40%, respectively. This reduction can be referred to the development of bending moment that increased the curvature and reduced the section rigidity. As a result, the lateral displacements increase and additional moment is produced, i.e. second order effect. This increases the mobilized stress on the section and cause failure at load levels lower than that of the pure axial loading. This can be confirmed by the very high strain values developed in GFRP in longitudinal and lateral directions. The strains recorded in GFRP at ultimate load levels were up to $-26297 \mu_s$ and $25961 \mu_s$, respectively, for specimen C11. Also, the specimens subjected to eccentric loading experienced considerably high deformability as seen from the longitudinal strain values. The response of eccentric loading is obviously more ductile than that of the pure axial loading. Similar observations were reported in literature for conventional concrete members [10&11]

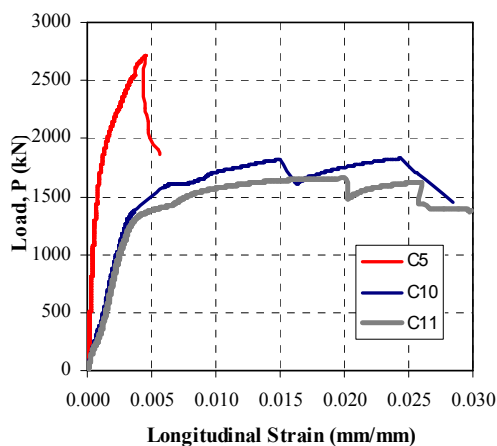


Figure (9): Effect of Load Eccentricity on Steel-Reinforced SCC Confined by GFRP

Referring to Figure 9, the introduction of load eccentricity caused the load-strain response to follow a saw tooth trend. After the drop of the load, the stresses redistributed on the cross section due to confinement and existence of steel reinforcement. As a result, the section restored its strength and the load increased. It can be said that load eccentricity has a

significant effect on SCC confined by GFRP. It reduced the ultimate capacity while it enhances the deformability.

6. Conclusions

The performance of self-compacting concrete confined using GFRP tube and subjected to compression loading was evaluated and the following conclusions were drawn:

1. The SCC confined with GFRP tube subjected to pure axial compression failed due to rupture of the GFRP followed by sudden crushing of concrete.
2. The failure of specimens subjected to eccentric loading was less brittle as the failure is due to combined axial compression and bending.
3. Confinement of SCC using GFRP tube resulted in notable enhancement in the structural performance of SCC. The confinement pressure from the GFRP enables the concrete core to withstand higher stresses and strains.
4. Gain in strength due to confinement with GFRP tube was up 50% and 37% for plain SCC and steel-reinforced SCC, respectively.
5. The presence of longitudinal reinforcement enhances the deformability as it transforms the behavior from that of brittle plain concrete to the more ductile reinforced concrete. However, increasing the percentage of longitudinal reinforcement from 1.5% to 2.16% resulted in marginal enhancement in both strength and deformability.
6. Reducing the diameter GFRP tube produces more effective confinement mechanism that enables the axially loaded SCC member to sustain higher stresses and strain.
7. Increasing the concrete compressive strength from 55.6 N/mm^2 to 100.5 N/mm^2 , increases the ultimate load and stiffness while it reduces the deformability of axially loaded SCC confined by GFRP. However, the increase in the ultimate load was only 59%, which is not proportional to the increase in the compressive strength of concrete by 81%.
8. Load eccentricity has a significant effect on the performance of SCC confined by GFRP. Generally, it reduces the ultimate capacity while it enhances the deformability and makes the behavior to be more ductile.
9. For the plain SCC confined by GFRP tube, introducing a load eccentricity of 25 mm resulted in a remarkable reduction in the ultimate capacity by 32% while the deformability increased by 55%.
10. For the steel-reinforced SCC confined by GFRP tube, increasing the load eccentricity from 0 to 25 mm and 40 mm reduced the ultimate load by 33% and 40%, respectively.

Acknowledgment

Acknowledgment is due to the staff of the materials laboratory at Housing and Building National Research Center in Egypt and the Future pipe Industries Company for their valuable help in this research.

References

1. ETS-2009, "Egyptian Technical Specifications for Self Compacting Concrete", Housing and Building National Research Center, Egypt, 2009.
2. Almusallam, T. H., "Behavior of Normal and High-strength Concrete Cylinders Confined with E-glass/Epoxy Composite Laminates", *Composites Part B: Engineering*, Vol. 138, pp. 629-639, 2007.
3. Issa, M. A., Alrousan, R. Z., and Issa, M. A., "Experimental and Parametric Study of Circular Short Columns Confined with CFRP Composites", *Journal of Composites for Construction*, ASCE, Vol. 13, No. 2, pp. 135-147 April 2009.
4. Bisby, L.A., Dent, A.J. S. and Green, M.F., "Comparison of Confinement Models for Fiber-Reinforced Polymer-Wrapped Concrete", *ACI Structural Journal*, Vol. 102, No. 1, pp. 199-213, January-February 2005.
5. Fahmy, M.F.M., and Wu, Z., "Evaluating and Proposing Models of Circular Concrete Columns Confined with Different FRP Composites", *Composites Part B*, Vol. 41, pp. 199-213, 2010.
6. El Chabib, H., Nehdi, M., and El Nagggar, M. H., "Behavior of SCC Confined in Short GFRP Tubes", *Journal of Cement & Concrete Composites*, Vol. 27, pp. 55-64, 2005.
7. ESS 4756-1 "Composition, Requirements and Compliance Criteria for Common Cement", Egyptian Organization for Standardization, Egypt, 2005.
8. ASTM C494/C494M-05a, "Standard Specification for Chemical Admixtures for Concrete", *ASTM Standards*, Vol. 04.02, 2005.
9. ASTM C157-02, "Standard Test Method for Length Change of Hardened Hydraulic Cement Mortar and Concrete", *ASTM Standards*, Vol. 04.02, 2006.
10. Csuka, B., and Kollar, L. P., "Analysis of FRP Confined Columns under Eccentric Loading", *Composites Structures*, Vol. 94, Issue 3, pp. 1106-1116, February 2012.
11. Wu, Y. F., and Jiang, C., "Effect of Load Eccentricity on the Stress-Strain Relationship of FRP-Confined Concrete Columns", *Composites Structures*, Vol. 98, pp. 228-241, April 2013.

12/11/2013